Numerically exact long-time behavior of nonequilibrium quantum impurity models

Emanuel Gull,[1] David R. Reichman,[2] and Andrew J. Millis[1]
[1]*Department of Physics, Columbia University, New York, New York 10027, USA*
[2]*Department of Chemistry, Columbia University, New York, New York 10027, USA*
(Received 4 August 2011; published 29 August 2011)

A Monte Carlo sampling of diagrammatic corrections to the noncrossing approximation is shown to provide numerically exact estimates of the long-time dynamics and steady-state properties of nonequilibrium quantum impurity models. This "bold" expansion converges uniformly in time and significantly ameliorates the sign problem that has heretofore limited the power of real-time Monte Carlo approaches to strongly interacting real-time quantum problems. The approach enables the study of previously intractable problems ranging from generic long-time nonequilibrium transport characteristics in systems with large on-site repulsion to the direct description of spectral functions on the real frequency axis in dynamical mean field theory.

DOI: 10.1103/PhysRevB.84.085134 PACS number(s): 05.10.Ln, 02.70.Ss, 02.70.Tt, 05.30.−d

I. INTRODUCTION

The nonequilibrium physics of strongly interacting quantum systems is a frontier research topic essential for fields ranging from the evolution of the early universe[1] to the current-voltage characteristics of single molecule devices.[2] A broad class of physically important nonequilibrium situations, including the physics of nanosystems coupled to leads,[3] adsorption of atoms on surfaces,[4] and magnetic impurities in metals,[5] can be expressed in terms of quantum impurity models: finite-size clusters of interacting fermions coupled to a noninteracting bath. These also serve as auxiliary problems in the dynamical mean field theory of equilibrium[6] and nonequilibrium[7] infinite lattice correlated systems.

Theoretical study of nonequilibrium physics has been hampered by a lack of effective and broadly applicable methods. Analytical approaches either involve uncontrolled approximations or have been restricted to weak interactions or to a special class of integrable systems.[8] Numerical approaches have also proven very limited. The standard quantum Monte Carlo approach is formulated in imaginary time and cannot be easily extended to the real-time situation needed for nonequilibrium problems. Numerical[9] and density matrix renormalization group[10] methods show promise but have not yet reached the level of generally useful tools.

Diagrammatic Monte Carlo evaluation of diagrammatic perturbation series has been very successful for equilibrium problems, producing important results in fields including quantum electrodynamics,[11] statistical mechanics,[12] and condensed-matter physics.[13–18] In these methods the Hamiltonian H is partitioned as $H = H_0 + H_1$ and the partition function Z at temperature T is expressed in an interaction representation and expanded in powers of H_1/T. The diagrammatic expansion order needed to obtain reliable results grows as $\langle H_1\rangle/T$, but in practice the method works down to temperatures that are much lower than the basic scales.[19]

In nonequilibrium problems the role of the partition function is played by the time evolution operator $K \sim \exp[iH_1t]$ and the role of inverse temperature is played by the time interval t to be studied. The factor of i means that a straightforward expansion suffers from a phase problem, which in practice severely limits the diagrammatic order which can be sampled and therefore the time intervals which can be studied. To date only relatively short times (up to ∼2–3 times the hybridization scale) could be accessed.[20–23]

In analytic many-body theory, partial resummation techniques are often used to sum up specific classes of diagrams. If the resummation captures enough of the physics, one may hope that an expansion around it will converge rapidly. In this paper we present a numerical formulation of an expansion around a partial resummation, applicable to nonequilibrium quantum impurity models and time-dependent dynamical mean field theory. We use the noncrossing approximation (NCA)[24,25] to perform the partial resummation, but we emphasize that the concepts and methods developed are general. We refer to this expansion as a "bold" expansion but note that it differs from "bold" algorithms which implicitly sample higher-order self-energy diagrams based on numerically computed lower-order diagrams.[26,27] Our method is based on a stochastic sampling of the full configuration space of all diagrams. It generalizes a previous expansion for equilibrium problems,[28] and it is numerically exact. It goes beyond previous work by including a treatment of the vertex corrections essential for the evaluation of expectation values and most importantly by converging *uniformly in time*: In contrast to the bare expansion, even the long-time behavior is adequately characterized by *finite* orders of bold perturbation theory. We present results for the steady-state density matrix and current, as well as the charge and magnetic relaxation times, which demonstrate that the method allows access to the nonequilibrium steady state for nontrivial interacting systems.

II. MODEL AND METHOD

We demonstrate the power of the method on the Anderson model with Hamiltonian

$$H_A = \sum_\sigma (\varepsilon_d + H\sigma) d_\sigma^\dagger d_\sigma + U n_\uparrow n_\downarrow + H_{\rm hyb} + H_{\rm lead}, \quad (1)$$

which describes a quantum dot with a single spin-degenerate orbital with correlation energy U hybridized to two leads labeled by $a = L, R$. The Hilbert space of the impurity consists of four states: $|0\rangle$, $|\uparrow\rangle$, $|\downarrow\rangle$, and $|\uparrow\downarrow\rangle$. H describes a magnetic field directed parallel to the spin quantization axis, $H_{\rm hyb} = \sum_{ka\sigma}[V_{ka\sigma} d_\sigma^\dagger c_{ka\sigma} + \text{H.c.}]$ parametrizes the

hybridization between the level and the leads, and $H_{\rm lead}$ describes the dynamics of the leads. Lead a is assumed to be in equilibrium at chemical potential μ_a and temperature T_a; the presence of two leads allows for departures from equilibrium parametrized by $\mu_L \neq \mu_R$ or $T_L \neq T_R$. An important parameter is the level width $\Gamma = \sum_{ka} V_{ka}^2 \delta(\varepsilon_{ka} - \mu_a)$. For our specific calculations we use the parametrization of Ref. 23 with $\mu_L = -\mu_R = V/2$, $\nu = 10 = \omega_c$.

We wish to compute time-dependent expectation values of operators $\hat{O}$ such as the dot charge (n) and spin (m) densities $n_\uparrow \pm n_\downarrow$ or the current flowing into the dot from (say) the left lead $J_L = i \sum_{k\sigma} [V_{kL\sigma} d_\sigma^\dagger c_{kL\sigma} - \text{H.c.}]$. These may be obtained from the time-dependent density matrix $\hat{\rho}(t)$ as

$$\langle \hat{O}(t_F) \rangle = \text{Tr}[\hat{O}\hat{\rho}(t_F)] = \text{Tr}[\hat{O} e^{-iH_A t_F} \hat{\rho}_0 e^{iH_A t_F}]. \qquad (2)$$

For nonequilibrium problems the only approach known to be reliable is to compute $\hat{\rho}(t)$ by evolving forward from an initial condition $\hat{\rho}_0$, as in the second term of Eq. (2).

We take $\hat{\rho}_0 = \hat{\rho}_0^{\rm dot} \otimes \hat{\rho}^{\rm lead}$ corresponding to decoupled impurity and leads and assume that $\hat{\rho}_0^{\rm dot}$ is diagonal in the occupation number basis. We evaluate Eq. (2) by writing the time evolution operators $e^{\pm i t H_A}$ in an interaction representation with respect to $H_{\rm hyb}$ and expanding powers of $H_{\rm hyb}$. The bare expansion produces diagrams of the form shown in Figs. 1(a) and 1(b). The presence of two time evolution operators in Eq. (2) means that two time contours are required, one running from an initial time $t = 0$ (left-hand side of the lower contour) to the measurement time t_F (right-hand side) and the other running back to initial time (left-hand side of the upper contour, with the label $2t_F$ indicating the total time interval along the double contour). Hybridization vertices $V_{ka\sigma} d_\sigma^\dagger c_{ka\sigma}$ ($V_{ka\sigma}^* c_{ka\sigma}^\dagger d_\sigma$) occurring at times $t_1 \cdots t_j$ are indicated by heavy (open) dots as in Ref. 28 and are connected by light lines displaced from the basic contour, indicating contractions of the lead (c) operators computed using $\hat{\rho}^{\rm lead}$ and by solid, wavy, or dashed lines indicating propagation in eigenstates of $H_{\rm dot}$.

A straightforward evaluation of Eq. (2) thus requires a sum over all diagrams, a sum over all contractions of lead operators, and an integral over all times. The sign problem arising from the powers of i limits diagrammatic Monte Carlo studies to situations where the mean perturbation order is $\lesssim 10$ (see Refs. 20–22) and for this reason only times $t \lesssim 2/\Gamma$ are accessible with this method.

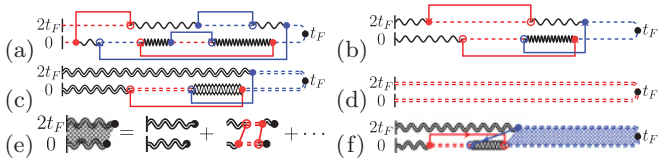

FIG. 1. (Color online) Diagrams arising in the bare hybridization and "bold" expansions of Eq. (1) on the Keldysh contour: Propagation in eigenstates of $H_{\rm dot}$ is described by wavy and dashed lines. Solid lines denote hybridization functions, and circles denote hybridization vertices. (a) NCA diagram. (b) Diagram containing crossing. (d) Bold propagator (dashed double line) which resums (a). (c) Diagram of bold expansion which resums diagrams including (b). Diagram (e) illustrates vertex resummations, and diagram (f) shows a bold vertex diagram.

Our bold method begins from the NCA, which integrates diagrams without "crossing" hybridization lines [e.g., Fig. 1(a)] using coupled integral equations. The correction diagrams are obtained along lines that are similar to those of the equilibrium algorithm of Ref. 28. Bare "atomic state" propagators and noncrossing hybridization lines are replaced by "bold" NCA propagators (denoted by heavy lines in Fig. 1). Diagrams with noncrossing hybridization lines contained in the underlying NCA propagators are not sampled. Thus, for example, the bold sampling process collapses Fig. 1(a) to Fig. 1(d), and Fig. 1(b) to Fig. 1(c).

Lines connecting one contour to another may be interpreted as vertex corrections to the operator placed at the measurement point t_F and to the initial density matrix. While they can be sampled directly, we find that it is best to resum noncrossing lines spanning a contour into NCA vertex corrections, and to replace the bare operator by a combination of the operator and its NCA vertex correction. An example is shown in Fig. 1(e) and the resulting "bold" version is shown in Fig. 1(f). Vertex corrections, especially for the vertices spanning the initial density matrix, significantly reduce the expansion order and the dynamic sign problem and allow us to perform an expansion about the NCA steady state.

Our Monte Carlo process is defined by moves which propose the addition or removal of vertices on either contour. The proposals are made without regard to whether or not the diagram is bold, but a proposed move which produces a diagram which is subsumable into a bold diagram is rejected. The procedure is exact because each bare diagram is contained in exactly one bold diagram. We combine diagrams in such a way that all terms are real,[22] so the phase problem becomes a sign problem. For computations of a given observable $\hat{O}$, the acceptance and rejection probabilities of a given move are determined from the absolute value of the contribution to $\langle \hat{O} \rangle$ and one measures $\langle \hat{O}\ \text{sign} \rangle / \langle \text{sign} \rangle$. The expectation value of the sign decays exponentially with the perturbation order considered and thus with the time interval to be studied. Management of the sign problem is a crucial issue in this and related methods.

We have found it useful to define a diagrammatic configuration at expansion order k (i.e., a set of vertices at times $t_1 \cdots t_{2k}$) as the sum of all contractions of lead operators consistent with the crossing condition. The lack of a Wick's theorem means that the sum must be performed explicitly. The exponential growth with perturbation order of the number of contractions sets a limit ~ 10 on the order which can be reached, but this limit is less severe in practice than the limit imposed by the sign.

III. RESULTS

Figure 2 shows the time dependence of the expectation value of the sign computed in an expansion of the current for the nonequilibrium Anderson model. The diamonds show the sign obtained from the bare hybridization expansion method of Refs. 20–22 and the circles show the sign obtained from a straightforward application of the bold method. (Essentially identical sign versus time curves are found for all parameters studied except that $\langle \text{sign} \rangle$ increases at very high $T \gtrsim \Gamma$.) The larger mean value of the sign at a given time in the bold

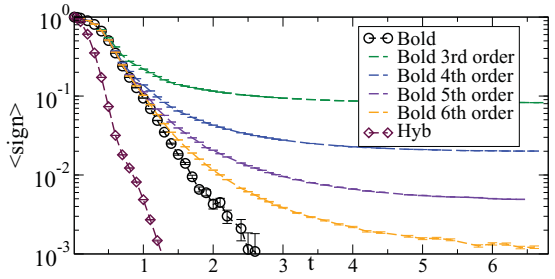

FIG. 2. (Color online) Average sign as a function of time in evaluation of expectation value of current for $U = 4, \beta = 50, H = 0, V = 5$. Bare expansion: diamonds. Bold expansion (all orders): circles. Other lines: Bold expansion truncated at orders 3–6.

method arises because fewer perturbation orders are needed to reach a solution. The exponential decrease of $\langle \text{sign} \rangle$ with time constrains the times that can be studied with finite resources. We see that the straightforward bold expansion can reach approximately twice as long a time as the bare expansion.

In contrast to equilibrium simulations, where the diagrams generated by the Monte Carlo process are typically the ones most important to the evaluation of the observable, we find that in the nonequilibrium situations considered here an unconstrained Monte Carlo exploration of bold diagrams generates many high-order diagrams which sum to zero in the observable. Thus we define a Monte Carlo process which considers only diagrams with perturbation order less than or equal to some value k, and then increase k until convergence is reached. For the cases studied here, $k \lesssim 8$ sufficed. Figure 2 shows that the mean sign decreases exponentially with increasing maximum perturbation order, but for a given perturbation order saturates at a nonzero value. We find that once the correct k is identified, the bold expansion can be arranged so that convergence is *uniform in time:* The mean perturbation order required to obtain a convergent result does not increase as the time interval is increased.

Convergence is poorest for spin-dependent properties of spin-imbalanced initial conditions; the main panel of Fig. 3 shows the slowest-converging case we have encountered so far. The straightforward bold expansion only converges out to times $t \approx 2$, the convergence with order is oscillatory, but by seventh order an acceptable convergence is reached, as can be seen from the coincidence of the sixth-, seventh-, and eighth-order results. The lower panel shows a more typical case, where convergence is monotonic and occurs by fourth order. The upper inset presents the contribution $w(t)$ made to the current at time t by the sum of all diagrams of a given order. We see that for this case diagrams of order $\gtrsim 5$ make no net contribution, but would be extensively sampled in a straightforward bold Monte Carlo calculation.

The much longer times accessible via the methods proposed here allow us to reach physically interesting steady states. Figure 4 shows the evolution of particular diagonal elements of the density matrix for different model parameters and starting from different initial conditions. The top and bottom traces ($U = 8$, $V = 1$, $H = 0.5$) show the evolution of the spin down (favored by H) and empty states starting from the initial condition in which the dot is in $|\downarrow\rangle$. The similar time scales in the evolution of the empty and singly occupied states

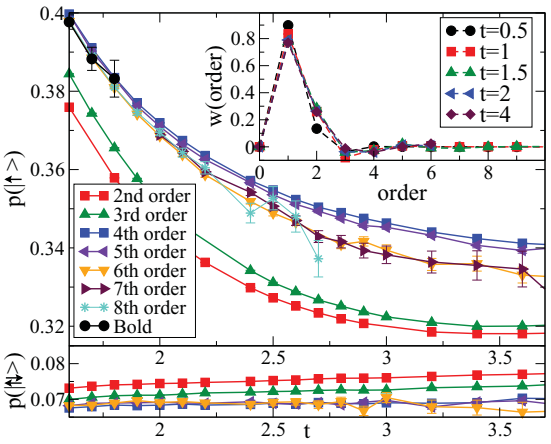

FIG. 3. (Color online) Order-by-order convergence for times $t = 1.5, \ldots, 4$. Upper panel: Spin imbalanced parameters, density expansion, $U = 4$, $V = 5$, state $|\uparrow\rangle$ (initial state $|\uparrow\rangle$), blowup to region of biggest differences. Lower panel: Typical case, $U = 8$, $V = 2$, $H = 0$, state $|\uparrow\downarrow\rangle$ starting from $|\uparrow\rangle$. Inset: Order-by-order contribution to current, for $U = 4$, $V = 5$ and times indicated.

show that the time dependence, which is rapid and is captured correctly by the bare and straightforward bold methods, is almost entirely due to charge relaxation. By contrast, the middle traces ($U = 4$, $V = 5$, $H = 0$) show the evolution of spin-up and spin-down states from a spin-polarized initial condition. A much slower spin relaxation is evident. The times $t \gtrsim 3$ required to access the steady state are only accessible by the methods proposed here. Similarly, Fig. 5 shows the time evolution of the current.

For a wide range of parameters and initial conditions we find that the magnetization relaxes exponentially to its steady-state value $m \sim \exp[-t/T_1]$. The inset of Fig. 4 compares the voltage and temperature dependence of the spin relaxation rate computed in the bold expansion and in the NCA. The latter systematically underestimates relaxation rates. Remarkably, the temperature dependence of T_1 is opposite at high and low voltages.

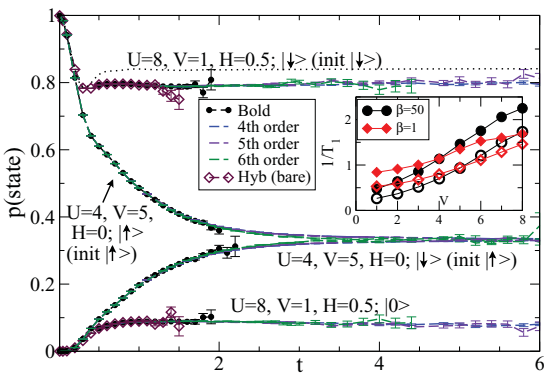

FIG. 4. (Color online) Time evolution of dot states from a specified initial condition, for parameters indicated calculated using bare expansion, bold expansion, and truncated bold expansion. Dotted line: NCA. Inset: Decay rate $1/T_1$ calculated for a nonequilibrium Anderson model at voltages and temperatures indicated for $U = 8$. Open symbols: NCA. Filled symbols: Bold.

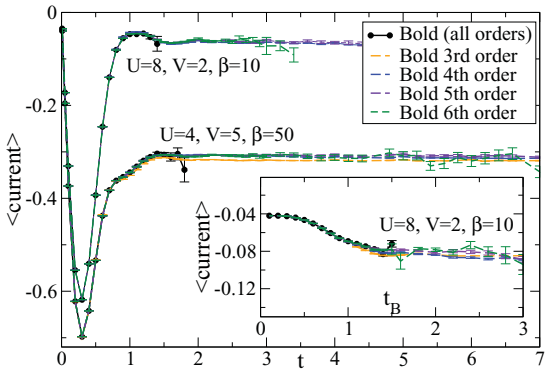

FIG. 5. (Color online) Time evolution of current for parameters indicated. Main panel: Starting from an empty dot. Inset: Starting from the NCA steady state.

The presence of analytically computed vertex functions in the algorithm allows improved access to the steady state by starting the bold computation from the density matrix corresponding to the NCA steady state rather than from a decoupled or noninteracting initial condition. In practice we use the NCA equations to propagate forward for a time t_0 from a decoupled state, after which the bold interactions are turned on and a further time t_B is studied. For the parameters we have studied the NCA density matrix is typically close to the true steady state, with the largest differences occurring for a nonzero field (dotted line, Fig. 4). Transients decay quickly. While NCA propagators and vertices are required for the entire time interval $t_F = t_0 + t_B$, the bold expansion needs only to operate over the much shorter time t_B. The inset of Fig. 5 shows the time evolution of the current from the NCA steady state to the numerically exact steady state for a representative choice of parameters. The large initial transient observed in the main panel is absent.

IV. CONCLUSION

In conclusion, we have developed a real-time diagrammatic method that enables a description of long-time and steady-state properties in nontrivial quantum impurity models over a wide range of interaction strengths and time scales. The approach is based on a systematic summation of terms contained in an expansion in powers of the hybridization portion of the Hamiltonian about a state described by an analytical resummation. This "bold expansion" is numerically exact, uniformly convergent, and greatly reduces the real-time sign problem that inhibits the study of long-time properties in "bare" continuous-time quantum Monte Carlo methods. We found that in many cases the noncrossing approximation provides reasonably accurate ($\lesssim$5%) estimates of the diagonal elements of the steady-state density matrix, but is less reliable for relaxation rates. A crucial open question is how far into the Kondo regime the method can be pushed.

ACKNOWLEDGMENTS

We thank P. Werner for many discussions and helpful insights. E.G. and A.J.M. are supported by NSF-DMR-1006282, and D.R.R. is supported by NSF-CHE-0719089. Calculations were performed on Brutus at ETH Zurich, using a code based on the ALPS (Ref. 29) library and at the Center for Nanophase Materials Sciences, which is sponsored at Oak Ridge National Laboratory by the Office of Basic Energy Sciences, US Department of Energy.

[1] J. Berges, in *IX Hadron Physics and VII Relativistic Aspects of Nuclear Physics: A Joint Meeting on QCD and QGP*, edited by M. Bracco, M. Chiapparini, E. Ferreira, and T. Kodama, AIP Conf. Proc. No. 739 (AIP, Melville, NY, 2004), p. 3.
[2] H. Song, M. A. Reed, and T. Lee, Adv. Mater. **23**, 1583 (2011).
[3] R. Hanson *et al.*, Rev. Mod. Phys. **79**, 1217 (2007).
[4] R. Brako and D. M. Newns, J. Phys. C **14**, 3065 (1981).
[5] P. W. Anderson, Phys. Rev. **124**, 41 (1961).
[6] A. Georges *et al.*, Rev. Mod. Phys. **68**, 13 (1996).
[7] M. Eckstein, M. Kollar, and P. Werner, Phys. Rev. B **81**, 115131 (2010).
[8] N. Andrei, K. Furuya, and J. H. Lowenstein, Rev. Mod. Phys. **55**, 331 (1983).
[9] F. B. Anders and A. Schiller, Phys. Rev. Lett. **95**, 196801 (2005).
[10] S. R. White and A. E. Feiguin, Phys. Rev. Lett. **93**, 076401 (2004).
[11] *Quantum Electrodynamics*, edited by T. Kinoshita (World Scientific, Singapore, 1990).
[12] A. W. Sandvik, in *Lectures on the Physics of Strongly Correlated Systems XIV: Fourteenth Training Course in the Physics of Strongly Correlated Systems*, edited by A. Avella and F. Mancini, AIP Conf. Proc. No. 1297 (AIP, Melville, NY, 2010), p. 135.
[13] N. V. Prokof'ev and B. V. Svistunov, Phys. Rev. Lett. **81**, 2514 (1998).
[14] E. Kozik *et al.*, Europhys. Lett. **90**, 10004 (2010).
[15] A. N. Rubtsov, V. V. Savkin, and A. I. Lichtenstein, Phys. Rev. B **72**, 035122 (2005).
[16] P. Werner, A. Comanac, L. deMedici, M. Troyer, and A. J. Millis, Phys. Rev. Lett. **97**, 076405 (2006).
[17] E. Gull *et al.*, Europhys. Lett. **82**, 57003 (2008).
[18] E. Gull *et al.*, Rev. Mod. Phys. **83**, 349 (2011).
[19] E. Gull, P. Werner, A. Millis, and M. Troyer, Phys. Rev. B **76**, 235123 (2007).
[20] L. Mühlbacher and E. Rabani, Phys. Rev. Lett. **100**, 176403 (2008).
[21] M. Schiró and M. Fabrizio, Phys. Rev. B **79**, 153302 (2009).
[22] P. Werner, T. Oka, and A. J. Millis, Phys. Rev. B **79**, 035320 (2009).
[23] P. Werner, T. Oka, M. Eckstein, and A. J. Millis, Phys. Rev. B **81**, 035108 (2010).
[24] H. Keiter and J. C. Kimball, Phys. Rev. Lett. **25**, 672 (1970).
[25] N. E. Bickers, Rev. Mod. Phys. **59**, 845 (1987).
[26] N. Prokof'ev and B. Svistunov, Phys. Rev. Lett. **99**, 250201 (2007).
[27] N. V. Prokof'ev and B. V. Svistunov, Phys. Rev. B **77**, 125101 (2008).
[28] E. Gull, D. R. Reichman, and A. J. Millis, Phys. Rev. B **82**, 075109 (2010).
[29] B. Bauer *et al.*, J. Stat. Mech.: Theory Exp. (2011) P05001.